UNIVERSITY KASDI MERBAH OUARGLA
Faculty of New Information Technologies and Communication
Department of Electronics and Telecommunication

ACADEMIC MASTER DISSERTATION

Domain: Sciences and Technologies
Branch: Telecommunications
Specialty: Systems of Telecommunications

TOPIC

Insulation Improvement in MIMO Antenna Using ENG Metamaterial Decoupling Structure

Presented by
- **Benazzouz Mohammed Mohyieddine**
- **Belal Mohammed**

Jury

Mr. Benatmane Khaled	MCB at UKM OUARGLA	President
Mr. Belhedri Abdelkrim	MCB at UKM OUARGLA	Examiner
Mr. Mekimah Boualem	MCA at UKM OUARGLA	Supervisor
Ms. Benderradji Houria Mihad	PHD at UKM OUARGLA	Co-Supervisor

University Year: 2025/2026

Abstract

This work presents the design and performance enhancement of a compact MIMO antenna operating at 60 GHz for millimeter-wave 5G communication systems. The primary objective is to improve isolation between closely spaced antenna elements using an ENG (Epsilon Negative) metamaterial decoupling structure. The proposed single antenna element achieves a reflection coefficient of $S_{11} = -28.51$ dB, a realized gain of 7.17 dBi, and a radiation efficiency of 92.68% at 60 GHz. A 2×1 MIMO antenna is then designed with an edge-to-edge spacing of 1.4 mm (0.28λ). Without isolation, the mutual coupling reaches approximately -18 dB. An ENG metamaterial unit cell is designed and characterized, exhibiting negative permittivity at the operating frequency. After integrating the ENG structure, the transmission coefficient S_{21} is significantly reduced from -18 dB to -50 dB, representing an isolation enhancement of 32 dB. Consequently, the Envelope Correlation Coefficient (ECC) remains approximately 4.06×10^{-8}, the Diversity Gain (DG) reaches 9.99 dB, the Channel Capacity Loss (CCL) remains below 0.4 bits/s/Hz, and the Total Active Reflection Coefficient (TARC) stays under -10 dB. These results confirm that the proposed ENG-based decoupling structure effectively suppresses mutual coupling and enhances MIMO performance, making it a suitable candidate for 60 GHz millimeter-wave communication applications.

Keywords: MIMO antenna, ENG metamaterial, mutual coupling, isolation enhancement, 60 GHz, 5G, millimeter-wave.

ملخص

يقدم هذا البحث تصميم وتحسين أداء هوائي MIMO مضغوط يعمل عند تردد 60 جيجاهرتز لأنظمة الاتصالات المليمترية من الجيل الخامس. الهدف الأساسي هو تحسين العزل بين عناصر الهوائي المتقاربة باستخدام بنية فك اقتران من نوع ENG (Epsilon Negative).

يحقق عنصر الهوائي المفرد قيمة معامل انعكاس قدرها $S_{11} = -23.41$ ديسيبل، وكسب قدره 17.7 dBi، وكفاءة إشعاع تصل إلى 92.68% عند تردد 60 جيجاهرتز. تم تصميم هوائي MIMO 1×2 بمسافة فاصلة بين العناصر تبلغ 4.1 مم (0.28λ). بدون عزل، يصل الاقتران المتبادل إلى حوالي -18 ديسيبل.

تم تصميم ودراسة خلية وحيدة من نوع ENG، حيث أظهرت نفاذية سالبة عند تردد التشغيل. بعد دمج الهيكل، انخفض معامل النقل S_{21} بشكل كبير من -18 ديسيبل إلى -50 ديسيبل، أي تحسن في العزل بمقدار 32 ديسيبل. ونتيجة لذلك، انخفض معامل ارتباط الغلاف (ECC) إلى 4.06×10^{-8}، ووصل كسب التنوع (DG) إلى 99.9 ديسيبل، وبقي فقدان سعة القناة (CCL) أقل من 4.0 bits/s/Hz، ومعامل الانعكاس النشط الكلي (TARC) تحت -10 ديسيبل.

تؤكد هذه النتائج أن بنية فك الاقتران المقترحة قادرة على قمع الاقتران المتبادل وتحسين أداء MIMO، مما يجعلها مناسبة لتطبيقات الاتصالات المليمترية عند تردد 60 جيجاهرتز.

الكلمات المفتاحية: هوائي MIMO، مادة ميتاماتيريال من نوع ENG، اقتران متبادل، تحسين العزل، 60 جيجاهرتز، الجيل الخامس، موجات مليمترية.

Resumé

Ce travail présente la conception et l'amélioration des performances d'une antenne MIMO compacte fonctionnant à 60 GHz pour les systèmes de communication millimétriques de la 5G. L'objectif principal est d'améliorer l'isolation entre les éléments d'antenne rapprochés en utilisant une structure de découplage à métamatériau ENG (Epsilon Negative). L'élément d'antenne unique proposé atteint un coefficient de réflexion de $S_{11} = -23.41$ dB, un gain réalisé de 7.17 dBi et une efficacité de rayonnement de 92.68% à 60 GHz. Une antenne MIMO 2×1 est ensuite conçue avec un espacement de 1.4 mm (0.28λ). Sans isolation, le couplage mutuel atteint environ -18 dB. Une cellule unitaire ENG est conçue et caractérisée, présentant une permittivité négative à la fréquence de fonctionnement. Après intégration de la structure ENG, le coefficient de transmission S_{21} est significativement réduit de -18 dB à -50 dB, soit une amélioration de l'isolation de 32 dB. Par conséquent, le coefficient de corrélation d'enveloppe (ECC) approximativement égal à 4.06×10^{-8}, le gain de diversité (DG) atteint 9.99 dB, la perte de capacité de canal (CCL) reste inférieure à 0.4 bits/s/Hz, et le coefficient de réflexion actif total (TARC) reste en dessous de -10 dB. Ces résultats confirment que la structure de découplage ENG proposée supprime efficacement le couplage mutuel et améliore les performances de l'antenne MIMO, ce qui en fait un candidat approprié pour les applications de communication millimétriques à 60 GHz.

Mots-clés : Antenne MIMO, métamatériau ENG, couplage mutuel, amélioration de l'isolation, 60 GHz, 5G, ondes millimétriques.

ACKNOWLEDGMENTS

In the name of Allah, the Most Gracious, the Most Merciful

All praise is due to Allah, Lord of all might and majesty, in Whose Hand lie dominion, permanence, and certainty. We thank Allah for enabling us to accomplish what we set out to do. May peace and blessings be upon our master Muhammad, peace be upon him.

To begin with, we extend our deep thanks and gratitude to our supervising professor, **Dr. Mekimah Boualem**, for the precise scientific guidance, continuous follow-up, and valuable advice he provided, all of which had a significant impact on the quality of this work.

We also express our highest appreciation and gratitude to **Dr. Benderradji Houria Mihad**, from whom we had the great fortune to learn. Her unwavering support, constant follow-up, and inspiring guidance, which she never withheld from us, were of great value. May Allah reward her on our behalf with all goodness.

We do not forget to extend our heartfelt thanks and gratitude **to all the professors of the Department of Electronics and Communications**, who exerted great efforts in teaching and guiding us, and played a major role in shaping our academic path and expanding our understanding.

We also express our sincere thanks and appreciation to **the College of Modern Information and Communication Technologies, especially the Department of Electronics**, for providing us with a motivating and supportive academic environment throughout our years of study.

May Allah reward you all on our behalf with the best of rewards and bless your knowledge and efforts.

DEDICATION

I dedicate this work to:

To my dear father and beloved mother, who gave me life, tenderness, guidance, and the courage to succeed. No words can truly express my deep love, gratitude, and appreciation for all the sacrifices you made for me. Through this humble dedication, I offer you my sincere thanks for your endless care, patience, prayers, and unconditional love with which you have always surrounded me.

To the memory of my late father, whose spirit continues to guide and inspire me. In moments when everything seemed impossible, thoughts of you gave me the strength to continue. This achievement is dedicated to you as much as it is to myself.

To my beloved mother, the light of my life, whose sincere prayers and limitless affection have always been my shelter and source of inspiration. I can never thank you enough for all your sacrifices and unwavering support.

To my dear brothers, and to the star of our home, my beloved sister, thank you for your constant encouragement, support, and love throughout my journey.

To my dear friends, who helped me build ideas, correct my mistakes, and encouraged me with valuable advice, humor, and continuous motivation throughout my years of study and during the preparation of this thesis. Your friendship and unforgettable support made this journey lighter, more meaningful, and truly memorable.

To all those who accompanied me throughout my life and left a positive mark on my path, thank you for your kindness and support. Special thanks go to my dear colleague for the cooperation, shared efforts, and encouragement throughout this work.

And to our esteemed supervising professors, who shared their knowledge, wisdom, and guidance with sincerity and dedication throughout this academic journey. Thank you for your valuable advice and continuous support.

With sincere love, appreciation, and gratitude to all.

Benazzouz Mohammed Mohyieddine and Belal Mohammed

Contents

Abstract i

Acknowledgements iii

Dedication v

GENERAL INTRODUCTION 2

CHAPTER I: MIMO SYSTEMS OVERVIEW 4

I.1 Introduction 4

I.2 Definition of MIMO 4

I.3 Operating Mechanism of MIMO Systems 5

I.4 Performance Benefits of MIMO Systems 5

I.4.1 Increased Channel Capacity 6

I.4.2 Improved Reliability 6

I.4.3 Diversity Gain 6

I.4.4 Multiplexing Gain 6

I.4.5 Better Spectral Efficiency 6

I.5 Types of MIMO Configurations 6

I.5.1 Single-Input Single-Output (SISO) 7

I.5.2 Single-Input Multiple-Output (SIMO) 7

I.5.3 Multiple-Input Single-Output (MISO) 7

I.5.4 Multiple-Input Multiple-Output (MIMO) 8

I.6 MIMO Antenna Parameters and Performance Metrics 9

I.6.1 Scattering Parameters (S-Parameters) 9

I.6.2 Envelope Correlation Coefficient (ECC) 10

I.6.3 Diversity Gain (DG) 11

I.6.4 Channel Capacity Loss (CCL) . . . 11
I.6.5 Total Active Reflection Coefficient (TARC) . . . 12
I.7 Techniques for Mutual Coupling Reduction . . . 12
I.7.1 Defected Ground Structure (DGS) . . . 13
I.7.2 Neutralization Line . . . 13
I.7.3 Electromagnetic Band Gap (EBG) . . . 13
I.7.4 Parasitic Elements . . . 13
I.7.5 Metamaterials . . . 14
Conclusion . . . 15

CHAPTER II: BACKGROUND ON METAMATERIALS **16**
II.1 Introduction . . . 16
II.2 Definition of Metamaterials . . . 16
II.3 Historical Background . . . 17
II.4 Electromagnetic Properties of Metamaterials . . . 17
II.5 Classification of Metamaterials . . . 18
II.6 ENG Metamaterial for Isolation Improvement . . . 20
Conclusion . . . 22

CHAPTER III: SIMULATION RESULTS AND PERFORMANCE EVALUATION **23**
III.1 Introduction . . . 23
III.2 Design methodology . . . 23
III.3 Analysis of the Single Antenna . . . 25
III.4 Proposed MIMO Antenna without Isolation Structure . . . 27
III.5 Design and Characterization of the ENG MTM Unit Cell . . . 29
III.6 MIMO Antenna with ENG Metamaterial Isolation Structure . . . 31
III.6.1 Parametric study of ENG position . . . 31
III.6.2 Comparative Isolation Analysis with and without the ENG Structure 31
III.7 MIMO Performance Metrics Analysis . . . 33
Conclusion . . . 36

Bibliography **38**

List of tables

1 Optimized dimensions of the proposed 60 GHz patch antenna. 25
2 Optimized dimensions of the proposed ENG unit cell. 30

List of figures

1 SISO, SIMO, MISO, and MIMO antenna configurations. 9

2 Different categories of electromagnetic materials, include DPS, ENG, MNG, and DNG according to the sign of ε and μ. 19

3 Flowcharts of the proposed design procedure: (a) single antenna design, (b) ENG unit cell design, and (c) MIMO antenna isolation enhancement. 24

4 Geometry of the proposed patch antenna: (a) front view and (b) back view. 25

5 Simulated performance of the proposed antenna: (a) S_{11}, and (b) gain and radiation efficiency. 26

6 Radiation patterns of the proposed patch antenna: (a) 3D radiation pattern and (b) 2D radiation patterns in the principal planes. 27

7 Geometry of proposed MIMO antenna without isolation structure. 28

8 Simulated S-parameters of the proposed MIMO antenna without unit cell. 28

9 Proposed ENG unit cell: (a) Geometry, and (b) Boundary conditions. . . 29

10 Simulated response of the proposed ENG unit cell: (a) S-parameters, and (b) extracted effective parameters. 30

11 Parametric study of ENG unit cell position: (a) geometry of proposed MIMO antenna with different ENG positions, and (b) simulated S_{21} for various ENG positions. 31

12 S-parameter comparison of MIMO antenna with and without ENG structure: (a) S_{11}, and (b) S_{21}. 32

13 Surface current distribution of the proposed MIMO antenna: (a) without the ENG structure, and (b) with the ENG metamaterial isolation structure. 33

14 2D radiation patterns of the proposed MIMO antenna with and without the ENG structure at 60 GHz: (a) Port 1 excitation and (b) Port 2 excitation. 34

15 Simulated MIMO performance metrics of the proposed antenna: (a) ECC and DG, and (b) CCL and TARC. 34

List OF Abbreviation

5G:	Fifth Generation
IoT:	Internet of Things
MIMO:	Multiple-Input Multiple-Output
mmWave:	Millimeter Wave
SISO:	Single-Input Single-Output
SIMO:	Single-Input Multiple-Output
MISO:	Multiple-Input Single-Output
ECC:	Envelope Correlation Coefficient
DG:	Diversity Gain
CCL:	Channel Capacity Loss
MEG:	Mean Effective Gain
TARC:	Total Active Reflection Coefficient
DGS:	Defected Ground Structure
EBG:	Electromagnetic Band Gap
SRR:	Split Ring Resonator
CSRR:	Complementary Split Ring Resonator
ENG:	Epsilon Negative
MNG:	Mu Negative
DNG:	Double Negative
DPS:	Double Positive
MTM:	Metamaterial
LHM:	Left-Handed Material
PEC:	Perfect Electric Conductor
PMC:	Perfect Magnetic Conductor
PTFE:	Polytetrafluoroethylene
RF:	Radio Frequency
GHz:	Gigahertz
dB:	Decibel
dBi:	Decibel Isotropic

GENERAL INTRODUCTION

The rapid evolution of modern wireless communication systems has accelerated the development of advanced technologies capable of supporting high data rates, low latency, massive connectivity, and efficient spectrum utilization. In this context, fifth-generation (5G) communication systems represent a major technological advancement, enabling emerging applications such as the Internet of Things (IoT), autonomous vehicles, smart cities, and high-definition multimedia services. To satisfy these demanding requirements, innovative antenna and electromagnetic technologies have become essential components in modern wireless networks [1, 2].

Among the most important technologies employed in 5G systems is Multiple-Input Multiple-Output (MIMO). By utilizing multiple antennas at both the transmitter and receiver sides, MIMO systems significantly improve channel capacity, communication reliability, and spectral efficiency. In addition, advanced techniques such as spatial multiplexing, spatial diversity, and beamforming further enhance wireless communication performance. However, the use of millimeter-wave (mmWave) frequency bands, introduces several technical challenges, including high propagation losses, increased sensitivity to obstacles, and strong mutual coupling between closely spaced antenna elements [3, 4].

To overcome these limitations, metamaterials have emerged as a promising solution in microwave and antenna engineering. Metamaterials are artificially engineered electromagnetic structures designed to exhibit properties not commonly found in natural materials, such as negative permittivity, negative permeability, and negative refractive index. These unique electromagnetic characteristics provide new possibilities for antenna miniaturization, bandwidth enhancement, gain improvement, and mutual coupling reduction in MIMO antenna systems [5, 6].

Depending on their electromagnetic properties, metamaterials can be classified into several categories, including Double Negative (DNG), Epsilon Negative (ENG), and Mu Negative (MNG) structures [7]. Among these categories, ENG metamaterials have attracted significant attention due to their capability to improve antenna performance while maintaining compact dimensions. Furthermore, metamaterial-based structures such as Split Ring Resonators (SRRs), Complementary Split Ring Resonators (CSRRs), and Electromagnetic Band Gap (EBG) structures are widely used to suppress unwanted electromagnetic coupling and enhance antenna isolation in compact MIMO systems [5, 8].

The main objective of this work is to investigate the design and performance enhancement of a compact MIMO antenna operating at millimeter-wave frequencies using metamaterial-based isolation techniques. This thesis presents both the theoretical background and the practical design aspects of MIMO antennas and metamaterials. The study focuses particularly on the implementation of an ENG metamaterial unit cell for improving antenna isolation and overall MIMO system performance in modern 5G wireless communication applications.

CHAPTER I: MIMO SYSTEMS OVERVIEW

I.1 Introduction

The rapid development of modern wireless communication systems, especially 5G networks, has increased the need for high-performance antenna technologies capable of providing high data rates, reliable communication, and efficient spectrum utilization. Among these technologies, Multiple-Input Multiple-Output (MIMO) systems play an important role in improving channel capacity and communication performance [9].

This chapter presents the theoretical background of MIMO technology. It introduces the basic concepts, operating mechanism, and different MIMO configurations. In addition, the main MIMO performance metrics such as S-parameters, ECC, DG, CCL, TARC, and MEG are discussed. The chapter also reviews the principal techniques used to reduce mutual coupling and improve antenna isolation, including DGS, EBG structures, parasitic elements, and metamaterials.

I.2 Definition of MIMO

Multiple-Input Multiple-Output (MIMO) is a wireless communication technology that utilizes multiple antennas at both the transmitter and receiver to improve communication performance. MIMO systems enable the simultaneous transmission and reception of multiple data streams over the same frequency band, which increases channel capacity, enhances communication reliability, and improves spectral efficiency without requiring additional bandwidth or transmission power [10, 11].

MIMO technology has become an essential component of modern wireless com-

munication systems, particularly in 5G networks, where high data rates, low latency, and reliable connectivity are required. By exploiting multipath propagation in wireless environments, MIMO systems significantly improve overall network performance and communication quality [11].

I.3 Operating Mechanism of MIMO Systems

MIMO systems operate by using multiple antennas at both the transmitter and receiver sides. At the transmitter, the input information is divided into several signals and transmitted simultaneously through different antenna elements. During propagation, the transmitted waves travel through multiple paths due to reflection, scattering, and diffraction in the wireless environment [12].

At the receiver side, signal processing algorithms are used to detect, separate, and decode the received signals. The availability of multiple propagation paths allows the receiver to process the incoming signals more efficiently [5, 13].

The operation of MIMO systems mainly relies on the following techniques:

- **Spatial Multiplexing:** allows the simultaneous transmission of multiple independent data streams through different antennas.
- **Spatial Diversity:** utilizes multiple propagation paths to reduce the impact of fading and signal degradation.
- **Beamforming:** controls the direction of transmitted signals toward the desired receiver to improve signal reception.

Modern 5G systems employ Massive MIMO technology, where a large number of antennas are integrated at base stations to support simultaneous wireless communications.

I.4 Performance Benefits of MIMO Systems

MIMO technology offers several performance advantages that make it highly suitable for modern wireless communication systems, especially 5G networks. The use of multiple antennas improves communication efficiency, transmission quality, and spectrum utilization [13].

I.4.1 Increased Channel Capacity

MIMO systems increase channel capacity by allowing the simultaneous transmission of multiple data streams over the same frequency band. This improves the overall data throughput without requiring additional bandwidth.

I.4.2 Improved Reliability

The presence of multiple transmission paths enhances communication reliability and reduces the effects of fading and interference. This leads to more stable wireless communication in complex propagation environments.

I.4.3 Diversity Gain

Diversity gain improves signal quality by reducing the probability of signal degradation during transmission. The use of multiple propagation paths increases link stability and communication robustness.

I.4.4 Multiplexing Gain

Multiplexing gain enhances data transmission efficiency through parallel signal transmission. This allows MIMO systems to support high-speed wireless communication services.

I.4.5 Better Spectral Efficiency

MIMO technology improves spectral efficiency by transmitting more information within the same bandwidth compared to conventional SISO systems. This efficient utilization of the spectrum is essential for modern high-capacity wireless networks.

I.5 Types of MIMO Configurations

Wireless communication systems can be classified according to the number of antennas used at the transmitter and receiver sides. These antenna configurations determine the communication performance, system complexity, and transmission efficiency. The

most common configurations are SISO, SIMO, MISO, and MIMO systems as depicted in Figure 1 [13, 14].

I.5.1 Single-Input Single-Output (SISO)

Single-Input Single-Output (SISO) is the simplest wireless communication configuration, where one transmitting antenna communicates with one receiving antenna. Traditional wireless systems mainly relied on SISO architectures due to their simple design and low implementation cost. However, SISO systems suffer from several limitations, including low channel capacity, poor spectral efficiency, and high sensitivity to fading and interference.

Because only one transmission path exists between the transmitter and receiver, the system performance strongly depends on the propagation environment [15]. Consequently, SISO systems are not suitable for modern communication requirements that demand high data rates and reliable connectivity [16].

I.5.2 Single-Input Multiple-Output (SIMO)

In Single-Input Multiple-Output (SIMO) systems, one transmitting antenna communicates with multiple receiving antennas. The main objective of this configuration is to improve signal reception quality and communication reliability through diversity techniques.

Since multiple receiving antennas capture different versions of the transmitted signal, the receiver can combine these signals to reduce fading effects and improve signal strength. SIMO systems are widely used in wireless receivers where reception reliability is more important than transmission capacity.

Compared with SISO systems, SIMO offers better resistance to multipath fading and interference while maintaining relatively low system complexity.

I.5.3 Multiple-Input Single-Output (MISO)

Multiple-Input Single-Output (MISO) systems employ multiple transmitting antennas and a single receiving antenna. In this configuration, the transmitter sends signals through several antennas simultaneously in order to improve transmission reliability and

signal quality.

MISO systems commonly utilize beamforming techniques, where transmitted signals are adjusted in phase and amplitude to direct signal energy toward the receiver. This improves coverage, reduces interference, and enhances communication stability.

MISO systems are particularly beneficial in wireless downlink communications, where base stations use multiple antennas to serve mobile users equipped with a single antenna.

I.5.4 Multiple-Input Multiple-Output (MIMO)

Multiple-Input Multiple-Output (MIMO) systems use multiple antennas at both the transmitter and receiver sides. This configuration provides the highest performance among all antenna configurations because it combines the advantages of spatial diversity and spatial multiplexing [17].

MIMO systems can simultaneously transmit several independent data streams through the same frequency band, significantly increasing channel capacity and spectral efficiency. In addition, the use of multiple propagation paths improves communication reliability and reduces the effects of fading and interference.

Modern 5G communication systems extensively rely on MIMO and Massive MIMO technologies to support high data rates, large user capacity, and low-latency wireless services [18].

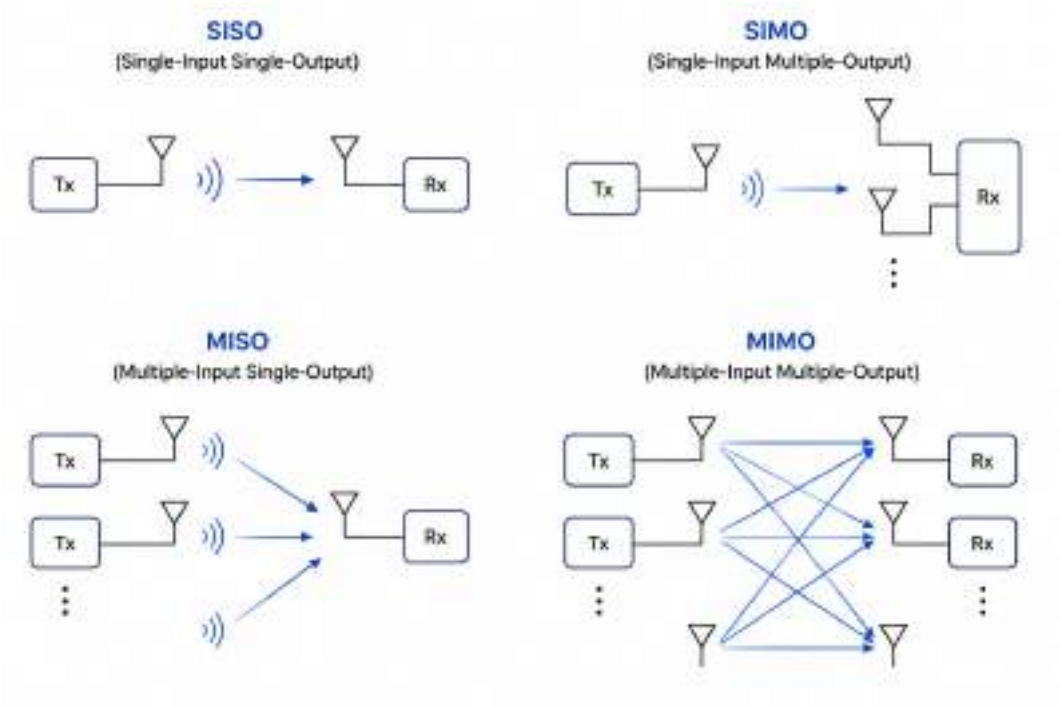


Figure 1: SISO, SIMO, MISO, and MIMO antenna configurations.

I.6 MIMO Antenna Parameters and Performance Metrics

The performance evaluation of MIMO antenna systems requires the analysis of several important parameters and metrics. These parameters are essential for determining the antenna efficiency, diversity capability, mutual coupling level, and overall communication performance. In modern 5G systems, accurate evaluation of these metrics is necessary to ensure reliable wireless communication and high spectral efficiency [19].

I.6.1 Scattering Parameters (S-Parameters)

Scattering parameters (S-parameters) are used to evaluate the electrical performance of MIMO antennas. They provide information about impedance matching and mutual coupling between antenna elements.

- **Reflection Coefficient** S_{11}

The parameter S_{11} represents the reflection coefficient at the antenna input port. It indicates the impedance matching quality of the antenna.

An S_{11} value below -10 dB is generally considered acceptable for efficient antenna operation.

◦ **Isolation Between Antenna Elements S_{21}**

The parameter S_{21} represents the transmission coefficient between antenna elements and is used to evaluate mutual coupling and isolation.

Low S_{21} values indicate good isolation between antenna elements. In practical MIMO systems, isolation values below -15 dB are preferred.

◦ **Mutual Coupling**

Mutual coupling is one of the major challenges in compact MIMO antenna systems. It refers to the undesired electromagnetic interaction between closely spaced antenna elements, where part of the electromagnetic energy radiated by one antenna is received by neighboring elements. This interaction modifies the current distribution on the antenna surfaces and affects their radiation behavior.

Several factors contribute to mutual coupling in MIMO antennas, including small spacing between antenna elements, surface wave propagation through the substrate, near-field electromagnetic interactions, shared ground planes, and radiation leakage between adjacent antennas. In compact antenna configurations, the coupling level becomes stronger as the distance between the elements decreases.

Mutual coupling negatively affects the overall performance of MIMO systems. It can reduce antenna efficiency, distort radiation patterns, increase signal correlation between antenna elements, and degrade impedance matching and bandwidth characteristics. In addition, high mutual coupling decreases diversity performance and channel capacity, which are important parameters for reliable wireless communication systems. Therefore, reducing mutual coupling is an essential requirement in the design of high-performance MIMO antennas.

I.6.2 Envelope Correlation Coefficient (ECC)

The Envelope Correlation Coefficient (ECC) is an important parameter used to evaluate the diversity performance of MIMO antenna systems. It measures the correlation between antenna elements and indicates the ability of the antennas to operate

independently during signal transmission or reception.

Low ECC values indicate a weak correlation between antenna elements, which improves diversity performance, reduces multipath fading effects, and enhances channel capacity and signal reliability. In contrast, high ECC values reflect strong coupling and poor diversity characteristics, leading to performance degradation in MIMO systems.

For efficient MIMO operation, ECC values are generally required to be lower than 0.5 [12].

The ECC can be calculated using the following equation:

$$ECC = \frac{\left|S_{ii}^{*}S_{ij} + S_{ji}^{*}S_{jj}\right|^{2}}{\left(1 - |S_{ii}|^{2} - |S_{ji}|^{2}\right)\left(1 - |S_{jj}|^{2} - |S_{ij}|^{2}\right)} \tag{1}$$

where:

- S_{ii} and S_{jj} are the reflection coefficients.
- S_{ij} and S_{ji} are the transmission coefficients.

I.6.3 Diversity Gain (DG)

Diversity Gain (DG) represents the improvement in communication reliability achieved by employing multiple antennas. It evaluates the ability of the antenna system to combat multipath fading using independent propagation paths.

A well-designed MIMO antenna system usually achieves a diversity gain close to 10 dB, indicating excellent diversity performance and stable communication quality [10].

$$DG = 10\sqrt{1 - (ECC)^{2}} \tag{2}$$

I.6.4 Channel Capacity Loss (CCL)

Channel Capacity Loss (CCL) measures the reduction in channel capacity caused by correlation and mutual coupling between antenna elements.

A low CCL value indicates efficient signal transmission and better spectrum utilization. In practical MIMO systems, CCL values below 0.4 bits/s/Hz are considered acceptable for high-performance communication systems.

Maintaining low CCL is particularly important in Massive MIMO systems where

many antenna elements operate simultaneously [12].

$$CCL = -\log_2\left(\det\left(\Psi_R\right)\right) \tag{3}$$

where,

$$\Psi_R = \begin{bmatrix} \Psi_{ii} & \Psi_{ij} \\ \Psi_{ji} & \Psi_{jj} \end{bmatrix}$$

$$\Psi_{ii} = 1 - \left(|S_{ii}|^2 + |S_{ji}|^2\right)$$

$$\Psi_{ij} = -\left(S_{ii}^* S_{ij} + S_{ji}^* S_{jj}\right)$$

$$\Psi_{ji} = -\left(S_{jj}^* S_{ji} + S_{ij}^* S_{ii}\right)$$

$$\Psi_{jj} = 1 - \left(|S_{jj}|^2 + |S_{ij}|^2\right)$$

I.6.5 Total Active Reflection Coefficient (TARC)

The Total Active Reflection Coefficient (TARC) evaluates the reflection performance of a MIMO antenna system when multiple antenna elements are excited simultaneously with different phases and amplitudes. Unlike conventional reflection coefficients, TARC considers the combined effect of all antenna ports and mutual coupling between elements. Low TARC values indicate good impedance matching and efficient operation under practical working conditions. For efficient MIMO operation, TARC values are generally expected to remain below -10 dB [17].

$$TARC = \sqrt{\frac{|S_{ii} + S_{ij}e^{j\theta}|^2 + |S_{ji} + S_{jj}e^{j\theta}|^2}{2}} \tag{4}$$

I.7 Techniques for Mutual Coupling Reduction

Reducing mutual coupling is one of the primary objectives in MIMO antenna design. Several techniques have been developed to improve antenna isolation while maintaining

compact size and high radiation performance [5].

I.7.1 Defected Ground Structure (DGS)

Defected Ground Structure (DGS) is a widely used technique for reducing mutual coupling in compact antenna arrays. It consists of introducing slots or defects in the ground plane to disturb surface current propagation. DGS structures help suppress coupling currents, improve isolation, and enhance impedance matching without significantly increasing antenna size. Additionally, DGS may improve bandwidth and reduce unwanted radiation effects.

I.7.2 Neutralization Line

Neutralization lines are conductive structures placed between antenna elements to cancel induced coupling currents. They create compensating current paths with opposite phases, thereby reducing electromagnetic interaction between antennas. This technique is simple, compact, and suitable for portable wireless devices where antenna spacing is limited.

I.7.3 Electromagnetic Band Gap (EBG)

Electromagnetic Band Gap (EBG) structures are periodic arrangements designed to prevent electromagnetic wave propagation within specific frequency ranges. When inserted between antenna elements, EBG structures suppress surface waves and reduce mutual coupling. EBG techniques are widely used in high-frequency and millimeter-wave antenna systems.

I.7.4 Parasitic Elements

Parasitic elements are passive metallic structures placed near antenna elements to control electromagnetic field distribution. These elements are not directly fed by the transmission line but interact with surrounding electromagnetic waves. Parasitic structures help improve isolation, modify radiation patterns, and reduce coupling effects between antennas.

I.7.5 Metamaterials

Metamaterials are artificial electromagnetic structures engineered to exhibit properties not commonly found in natural materials [20, 21, 22, 23]. These structures can manipulate electromagnetic wave propagation and improve antenna isolation performance.Common metamaterial-based isolation techniques include:

- Split Ring Resonators (SRR)
- Complementary Split Ring Resonators (CSRR)
- Electromagnetic Band Gap structures (EBG)

These techniques effectively suppress unwanted electromagnetic coupling and improve MIMO antenna performance without significantly increasing antenna dimensions.

Conclusion

This chapter has presented the theoretical background of MIMO antenna systems used in modern wireless communication networks. The fundamental concepts of MIMO technology, the operating mechanism, and the main performance benefits have been discussed. Different MIMO antenna configurations, including SISO, SIMO, MISO, and MIMO systems, were also introduced. In addition, important MIMO antenna performance metrics such as S-parameters, ECC, DG, CCL, TARC,and MEG were presented to evaluate antenna efficiency, isolation, and diversity performance. Finally, several mutual coupling reduction techniques, including DGS, EBG, parasitic elements, neutralization lines,and metamatrials were reviewed to improve antenna isolation and overall MIMO system performance. The theoretical concepts discussed in this chapter provide the necessary foundation for the design and analysis of high-performance MIMO antenna systems for modern 5G and millimeter-wave communication applications.

CHAPTER II: BACKGROUND ON METAMATERIALS

II.1 Introduction

Metamaterials have attracted considerable attention in modern electromagnetic and antenna engineering due to their unique properties that are not commonly available in natural materials. These artificial structures are composed of periodic unit cells designed to manipulate electromagnetic wave propagation in a controlled manner. As a result, metamaterials have become widely used in microwave and wireless communication applications.

This chapter presents the theoretical background of metamaterials and their applications in antenna systems. It introduces the basic concepts of metamaterials, their classifications, and the main electromagnetic parameters used to characterize their behavior.

II.2 Definition of Metamaterials

The word “meta” comes from the Greek language and means “beyond”. Therefore, metamaterials can be defined as artificial materials whose electromagnetic properties go beyond those of conventional natural materials. They are engineered using periodic unit cells that are much smaller than the operating wavelength. Unlike ordinary materials, metamaterials may exhibit unusual electromagnetic properties such as negative permittivity, negative permeability, or negative refractive index. These properties allow for better control of electromagnetic wave propagation and radiation behavior.

II.3 Historical Background

The concept of metamaterials was first introduced theoretically in 1968 by the Russian physicist Victor Veselago. He investigated materials possessing simultaneously negative permittivity and negative permeability, and predicted that such materials could exhibit a negative refractive index. At that time, these properties were only theoretical because no natural material was known to exhibit such electromagnetic behavior.

Later, significant progress in metamaterial research was achieved through the work of Pendry, who proposed artificial periodic structures capable of producing negative electromagnetic parameters. Metallic wire arrays were introduced to realize negative permittivity, while Split Ring Resonators (SRRs) were developed to achieve negative permeability. With the advancement of electromagnetic simulation tools and fabrication technologies, metamaterials have become widely used in microwave and antenna engineering applications. Today, they are extensively investigated for applications such as antenna miniaturization, bandwidth enhancement, gain improvement, and mutual coupling reduction in MIMO antenna systems.

II.4 Electromagnetic Properties of Metamaterials

The electromagnetic behavior of metamaterials is mainly characterized by three important parameters: permittivity, permeability, and refractive index. These parameters determine how electromagnetic waves propagate through the material.

II.4.1 Permittivity (ε)

Permittivity represents the ability of a material to respond to an electric field. It describes how electric energy is stored within the material. In conventional materials, the permittivity is usually positive. However, metamaterials can be engineered to exhibit negative permittivity over specific frequency ranges. Materials with negative permittivity are commonly realized using periodic metallic wire structures. These structures modify the movement of electrons and create an effective electromagnetic response that does not naturally exist. Negative permittivity is widely used in antenna miniaturization and gain enhancement applications.

II.4.2 Permeability (μ)

Permeability describes the response of a material to a magnetic field. It determines how magnetic energy propagates through the medium. Similar to permittivity, permeability in natural materials is generally positive, while metamaterials can exhibit negative permeability under certain operating conditions. Negative permeability is typically achieved using resonant structures such as Split Ring Resonators (SRRs) or Swiss-roll structures. These resonators generate magnetic responses capable of producing negative permeability around resonance frequencies. Metamaterials with negative permeability are frequently used for isolation improvement, beam focusing, and electromagnetic wave control in antenna systems.

II.4.3 Refractive Index (n)

The refractive index determines how electromagnetic waves propagate through a medium. In metamaterials, the refractive index depends on both permittivity and permeability. When both parameters become negative simultaneously, the refractive index also becomes negative. A negative refractive index leads to unusual electromagnetic phenomena such as reverse wave propagation, inverse Snell's law, and backward phase propagation. These unique characteristics make metamaterials highly attractive for advanced microwave and antenna applications. The refractive index of metamaterials is generally expressed as:

$$n = \sqrt{\varepsilon_{eff}\mu_{eff}} \tag{5}$$

where ε_{eff} is the effective permittivity and μ_{eff} is the effective permeability of the metamaterial structure.

II.5 Classification of Metamaterials

Metamaterials are commonly classified according to the signs of their effective permittivity (ε) and permeability (μ) as shown in Figure 2. Four main categories exist: Double Positive (DPS), Double Negative (DNG), Epsilon Negative (ENG), and Mu Negative (MNG). Each category exhibits different electromagnetic characteristics, which directly

influence electromagnetic wave propagation behavior.

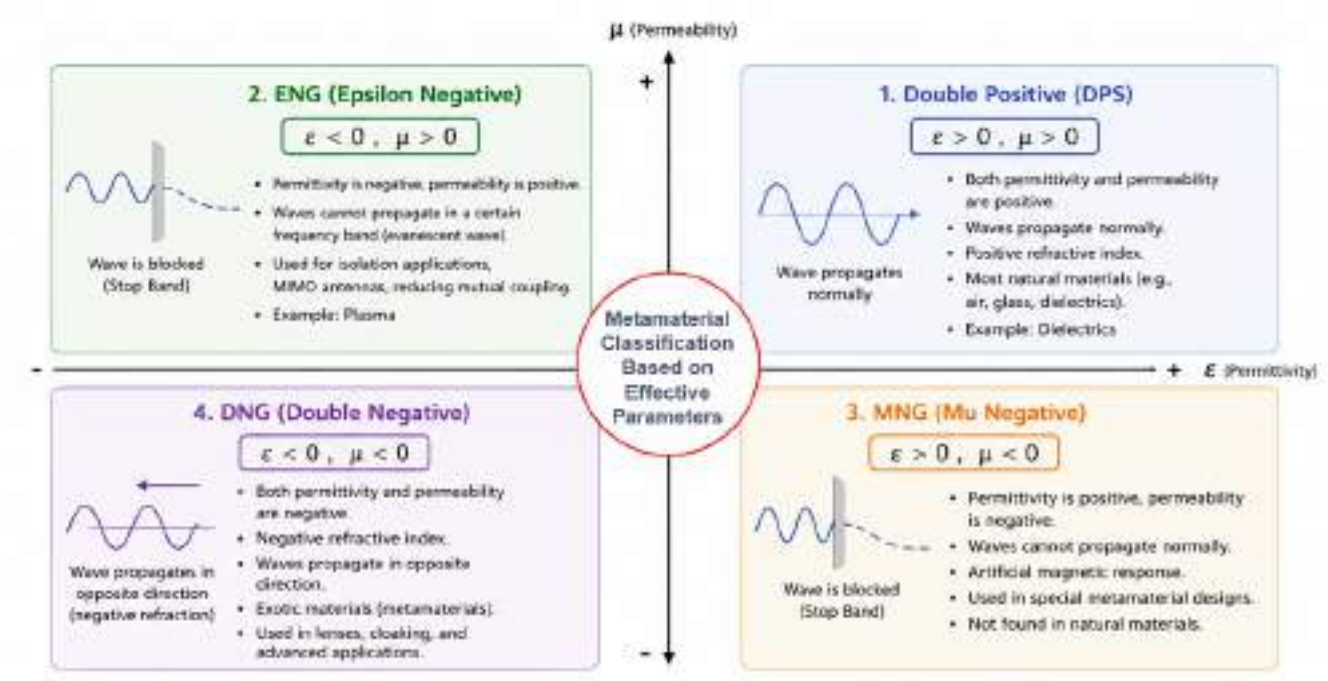


Figure 2: Different categories of electromagnetic materials, include DPS, ENG, MNG, and DNG according to the sign of ε and μ.

II.5.1 Double Positive (DPS)

Double Positive (DPS) materials are conventional materials in which both permittivity and permeability are positive: $\varepsilon > 0, \quad \mu > 0$. Most natural dielectric materials belong to this category. Electromagnetic waves propagate normally through DPS materials with positive refractive index characteristics.

II.5.2 Double Negative (DNG)

Double Negative (DNG) metamaterials are structures where both permittivity and permeability become negative simultaneously: $\varepsilon < 0, \quad \mu < 0$. These materials exhibit negative refractive index behavior and are also known as left-handed materials (LHM). DNG metamaterials are usually realized by combining structures that provide negative permittivity and negative permeability together, such as metallic wire arrays and SRR resonators. DNG metamaterials are widely used for antenna miniaturization, bandwidth enhancement, and gain improvement.

II.5.3 Epsilon Negative (ENG)

Epsilon Negative (ENG) metamaterials are characterized by negative permittivity and positive permeability: $\varepsilon < 0, \quad \mu > 0$. ENG materials are generally obtained using thin metallic wire structures. They are particularly useful in antenna engineering applications, such as size reduction, gain enhancement, and filtering structures. In modern antenna systems, ENG metamaterials are commonly employed for isolation enhancement and compact antenna design.

II.5.4 Mu Negative (MNG)

Mu Negative (MNG) metamaterials possess positive permittivity and negative permeability: $\varepsilon > 0, \quad \mu < 0$. Negative permeability is generally achieved using resonant magnetic structures such as Split Ring Resonators (SRRs). MNG metamaterials are frequently utilized for electromagnetic wave suppression, antenna isolation improvement, and beam manipulation applications. These structures are especially important in MIMO antenna systems where reducing mutual coupling between antenna elements is essential for improving overall communication performance.

II.6 ENG Metamaterial for Isolation Improvement

Among the different metamaterial categories, ENG and MNG structures are widely used in antenna applications due to their ability to suppress electromagnetic wave propagation. This property makes them suitable for reducing mutual coupling and improving isolation in compact MIMO antenna systems. The propagation constant inside ENG and MNG metamaterials can be expressed as [24]:

$$K = \beta - j\gamma \tag{6}$$

where,

- K: Wave number
- β: Propagation constant
- γ: Attenuation coefficient
- ω: Angular frequency

- ε, μ: Effective permittivity and permeability

  The wave number is given by:

$$k = \omega\sqrt{\varepsilon\mu} \tag{7}$$

When either ε or μ becomes negative, electromagnetic waves become strongly attenuated, creating a stop-band region that blocks wave propagation. In this work, an ENG metamaterial structure is employed as an isolation element to improve the isolation performance of the proposed MIMO antenna system.

Conclusion

This chapter has presented an overview of metamaterials and their importance in modern microwave and antenna engineering applications. The fundamental concepts of metamaterials, their historical development, and their main electromagnetic properties, including permittivity, permeability, and refractive index, have been discussed. In addition, the different classifications of metamaterials, such as DPS, DNG, ENG, and MNG structures, have been introduced. The unique electromagnetic characteristics of metamaterials make them highly suitable for antenna miniaturization, gain enhancement, and isolation improvement in MIMO systems. The theoretical concepts discussed in this chapter provide the necessary foundation for the design and analysis of the proposed metamaterial unit cell presented in the next chapter.

CHAPTER III: SIMULATION RESULTS AND PERFORMANCE EVALUATION

III.1 Introduction

This chapter presents the simulation results and performance analysis of the proposed 60 GHz MIMO antenna. First, the single antenna element is designed and analyzed to validate its impedance matching and radiation characteristics. Then, the MIMO configuration is investigated before introducing the ENG metamaterial isolation structure. Finally, the influence of the ENG unit cell on isolation level and MIMO performance metrics is presented and discussed.

III.2 Design methodology

The design methodology adopted in this work is illustrated in Fig. 3 The first stage consists of designing a compact single patch antenna operating at 60 GHz on a PTFE substrate with a relative permittivity of 2.1 and a thickness of 0.254 mm. The antenna geometry is optimized to achieve satisfactory impedance matching, high gain, and good radiation efficiency at the target frequency. Electromagnetic simulations are carried out using CST Studio Suite 2024 to evaluate the antenna performance in terms of reflection coefficient (S_{11}), gain, and efficiency. If the desired performance is not achieved, the antenna dimensions are further adjusted until the required characteristics are obtained.

Its electromagnetic response is analyzed through the extraction of the scattering parameters and effective parameters, effective permittivity (ε_r). If the desired ENG

behavior is not observed around 60 GHz, the unit-cell dimensions are optimized and the simulation process is repeated until the targeted response is achieved.

In the final stage, a 2×1 MIMO antenna configuration is constructed using two identical patch antenna elements separated by a compact spacing. The initial MIMO structure is first analyzed without any isolation mechanism to evaluate the mutual coupling characteristics. Subsequently, the proposed ENG unit cell is integrated between the antenna elements, and a parametric study is performed to determine its optimal position. The transmission coefficient (S_{21}) is used as the primary indicator of isolation performance during the optimization process. Once the optimum position is identified, the final MIMO antenna is evaluated in terms of isolation and diversity performance using the scattering parameters and MIMO metrics. This systematic design procedure enables the development of an ENG-based MIMO antenna with significantly improved isolation and enhanced overall performance at 60 GHz.

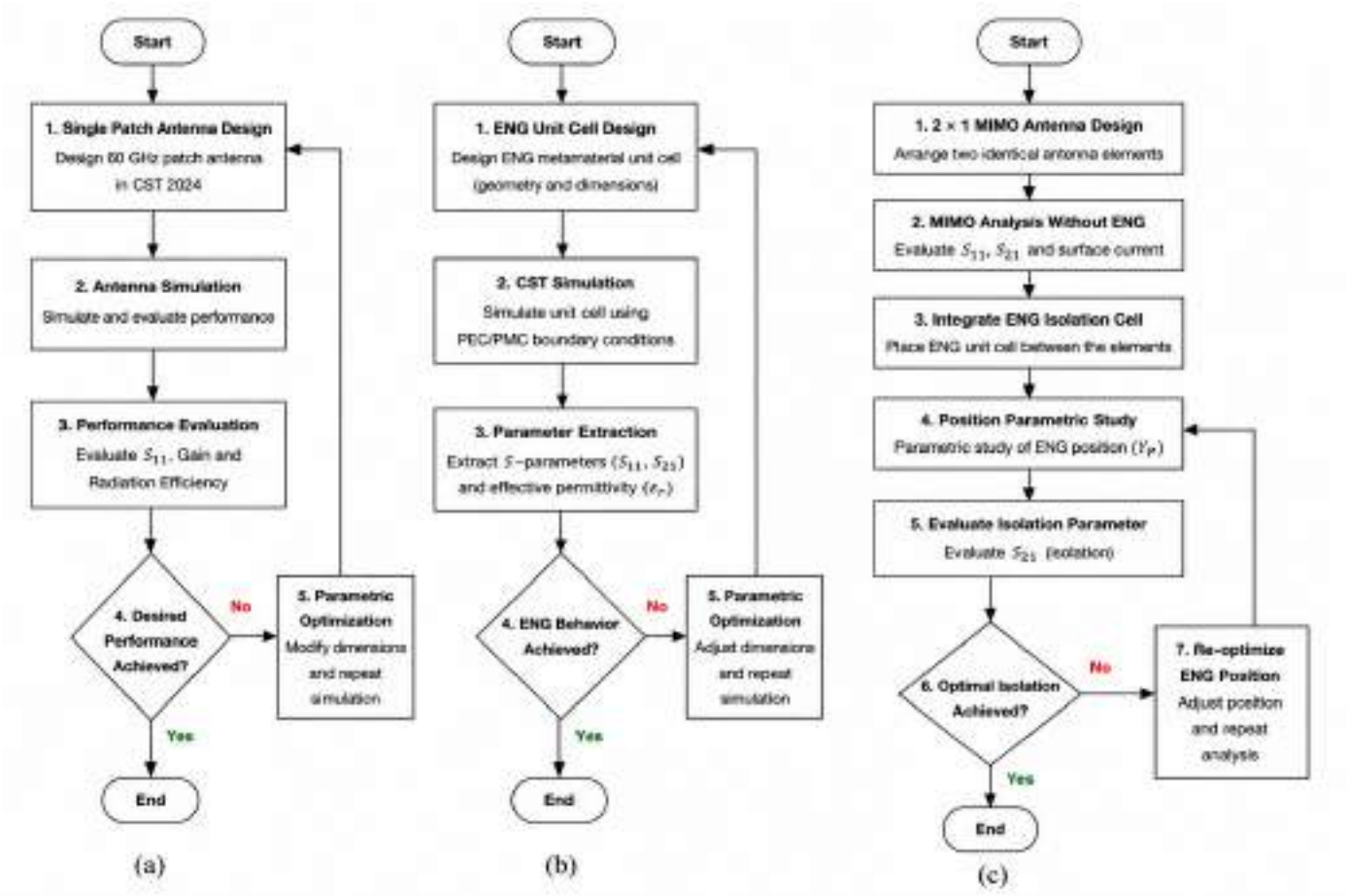
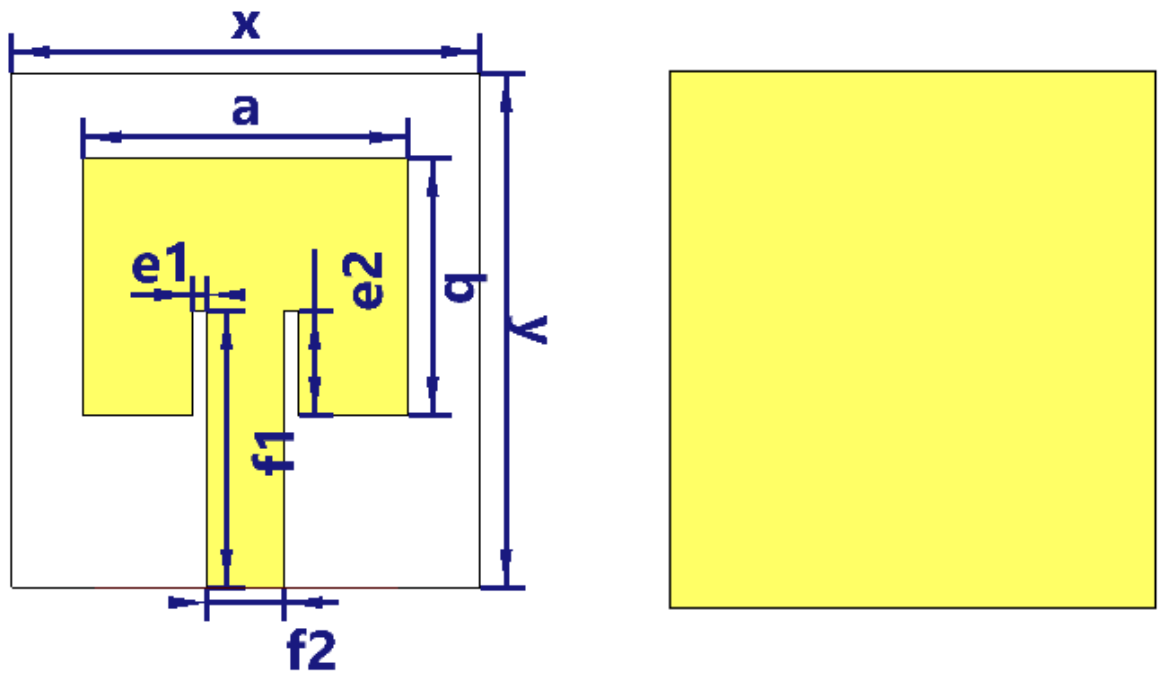


Figure 3: Flowcharts of the proposed design procedure: (a) single antenna design, (b) ENG unit cell design, and (c) MIMO antenna isolation enhancement.

III.3 Analysis of the Single Antenna

The geometry of the proposed patch antenna operating at 60 GHz is depicted in Figure. 4a. The initial dimensions of the antenna were adopted from a previously reported design in the literature [4] and subsequently optimized to satisfy the requirements of the present work. The antenna is excited by a 50 Ω microstrip feed line in order to achieve proper impedance matching with standard RF circuitry. The proposed structure occupies compact overall dimensions of $0.98\lambda \times 1.08\lambda$ (4.9 mm × 5.4 mm), which makes it suitable for millimeter-wave wireless communication applications. The antenna is fabricated on a PTFE substrate characterized by a relative permittivity of $\varepsilon_r = 2.1$, a thickness of 0.254 mm, and a full ground plane on the bottom side of the substrate as illustrated Figure. 4b. The adopted antenna geometry has been carefully optimized to ensure stable resonance behavior around the targeted 60 GHz frequency band.



(a) (b)

Figure 4: Geometry of the proposed patch antenna: (a) front view and (b) back view.

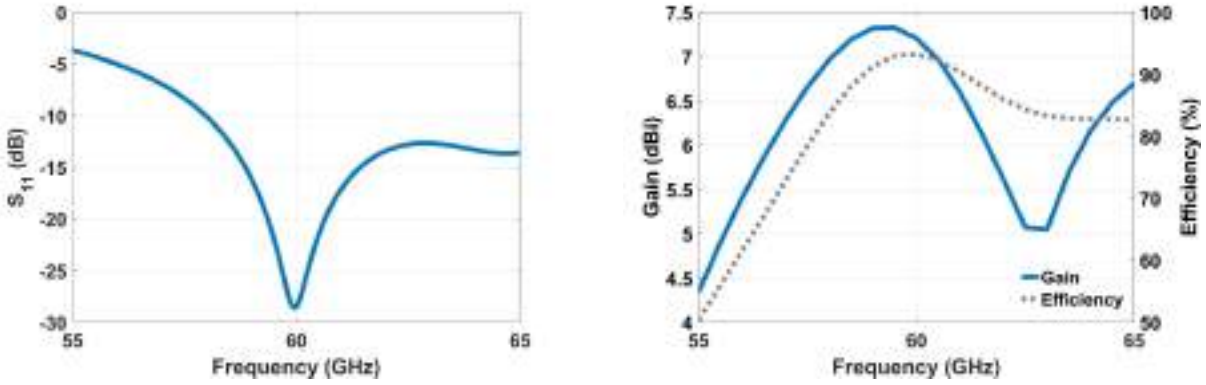
Table 1: Optimized dimensions of the proposed 60 GHz patch antenna.

Parameter	x	y	a	b	e_1	e_2	f_1	f_2
Value (mm)	4.900	5.400	3.415	2.700	0.150	1.100	2.900	0.810

The simulated reflection coefficient of the proposed antenna is presented in Fig-

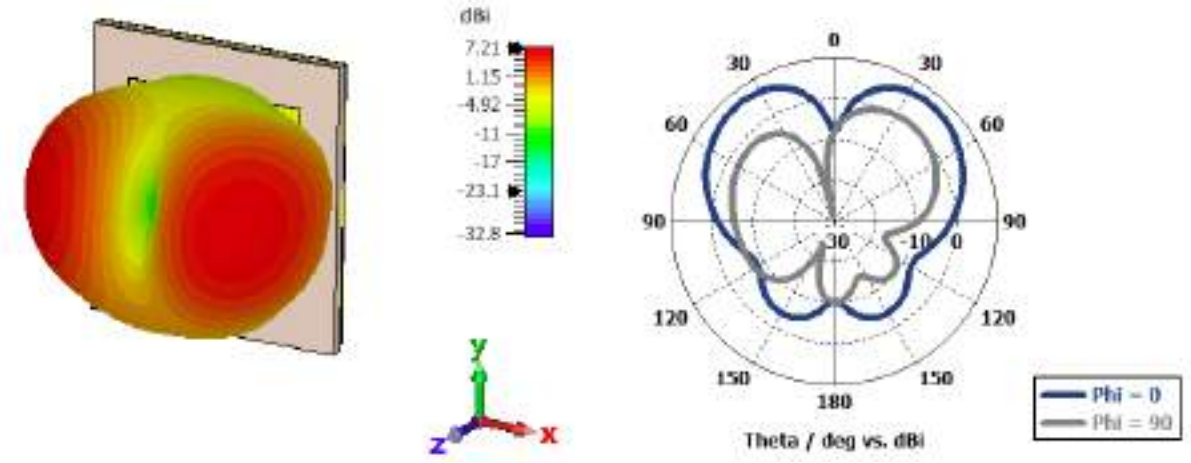
ure 5a. The antenna demonstrates satisfactory impedance matching characteristics, achieving a minimum reflection coefficient of $S_{11} = -28.51$ dB at the target frequency of 60 GHz. This value is substantially below the conventional -10 dB threshold, indicating efficient power transfer between the feed network and the radiating element. Furthermore, the antenna provides a -10 dB impedance bandwidth extending from 57.97 GHz to beyond 65 GHz, corresponding to an absolute bandwidth greater than 7.03 GHz. This bandwidth fully encompasses the intended 60 GHz operating frequency, making the proposed design suitable for millimeter-wave communication applications.

Figure 5b illustrates the simulated gain and radiation efficiency of the proposed antenna. A realized gain of 7.17 dBi is attained at the resonant frequency. Furthermore, the total radiation efficiency is approximately 92.68%, confirming the proposed design ability to efficiently radiate the accepted input power with minimal losses. These findings indicate that the proposed antenna is well-suited for high-performance millimeter-wave communication systems.



(a) (b)

Figure 5: Simulated performance of the proposed antenna: (a) S_{11}, and (b) gain and radiation efficiency.



(a) (b)

Figure 6: Radiation patterns of the proposed patch antenna: (a) 3D radiation pattern and (b) 2D radiation patterns in the principal planes.

Figure 6a presents the three-dimensional radiation pattern of the proposed patch antenna at the operating frequency of 60 GHz. It can be observed that the antenna exhibits a directional broadside radiation characteristic with a maximum realized gain of approximately 7.21 dBi. This behavior confirms the ability of the proposed antenna to effectively concentrate the radiated power toward the desired direction, making it suitable for millimeter-wave communication applications.

The corresponding two-dimensional radiation patterns for the principal cuts, $\phi = 0°$ and $\phi = 90°$, are depicted in Figure 6b. The radiation pattern associated with $\phi = 0°$ exhibits the dominant radiation lobe with a peak gain of approximately 6.93 dBi and a 3-dB beamwidth of about 49°, indicating a directional radiation characteristic. In contrast, the $\phi = 90°$ cut presents a lower radiation level, illustrating the variation of the radiated field distribution in different observation planes. Overall, the proposed antenna maintains stable directional radiation characteristics with an adequate gain level for 60 GHz wireless communication systems.

III.4 Proposed MIMO Antenna without Isolation Structure

Figure 7 illustrates the geometry of the proposed 2×1 MIMO antenna without any isolation structure. The configuration comprises two identical patch antenna elements

arranged symmetrically above a common full ground plane, with an edge-to-edge separation of $d = 1.4$ mm, corresponding to approximately 0.28λ at 60 GHz. This compact spacing is selected to achieve a reduced overall footprint suitable for millimeter-wave applications. Nevertheless, such close proximity may intensify electromagnetic interaction between the radiating elements, thereby inducing mutual coupling effects.

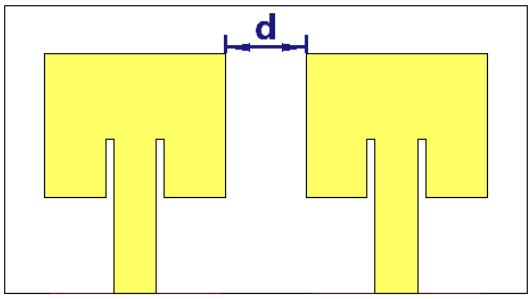


Figure 7: Geometry of proposed MIMO antenna without isolation structure.

Figure 8 presents the simulated S-parameters of the proposed MIMO antenna without any isolation structure. The antenna maintains acceptable impedance matching around 60 GHz, with S_{11} below -10 dB. However, the transmission coefficient S_{21} reaches approximately -18 dB, indicating the existence of mutual coupling between the closely spaced antenna elements.

This coupling is mainly attributed to near-field interaction and surface-wave propagation between the radiating patches, which degrade the isolation performance of the MIMO system.

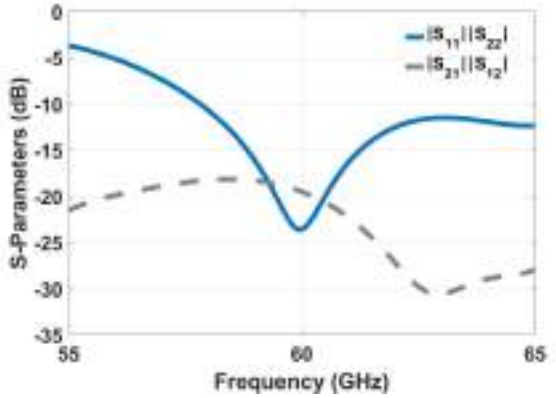
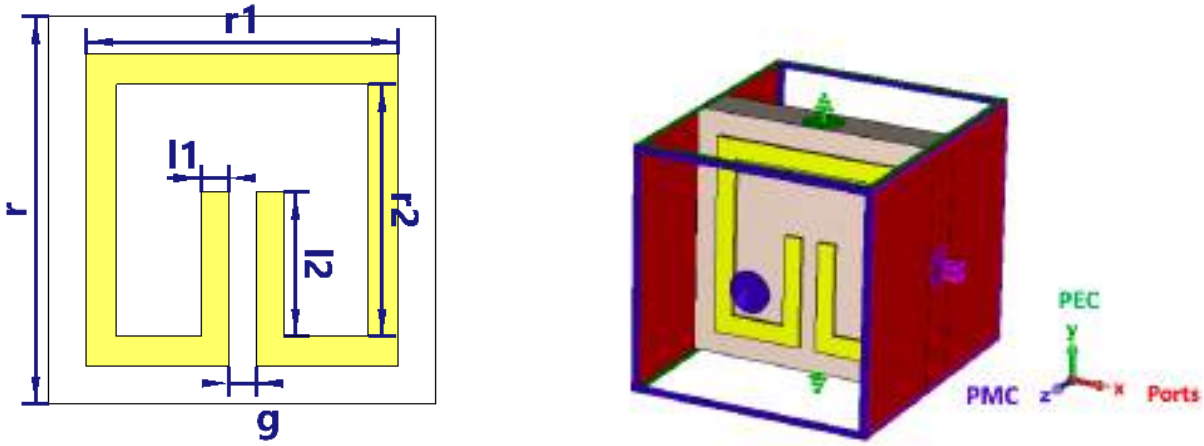


Figure 8: Simulated S-parameters of the proposed MIMO antenna without unit cell.

III.5 Design and Characterization of the ENG MTM Unit Cell

Figure 9a illustrates the geometry and optimized dimensions of the proposed ENG metamaterial unit cell, designed to operate around 60 GHz. The structure is implemented on a PTFE substrate with relative permittivity $\varepsilon_r = 2.1$ and substrate thickness $h = 0.254$ mm at the operating frequency. The optimized geometrical parameters of the unit cell are summarized in the figure caption. The proposed structure is designed to produce a compact stop-band response capable of suppressing electromagnetic wave propagation and reducing mutual coupling between closely spaced MIMO antenna elements.

Figure 9b presents the boundary conditions employed for the electromagnetic characterization of the proposed unit cell. Perfect Electric Conductor (PEC) boundaries are applied along one pair of opposite walls, while Perfect Magnetic Conductor (PMC) boundaries are assigned to the orthogonal walls. In addition, waveguide ports are positioned along the propagation direction to evaluate the transmission and reflection characteristics of the metamaterial structure. This simulation configuration enables accurate extraction of the electromagnetic response and effective parameter characteristics around the target frequency band.



(a) (b)

Figure 9: Proposed ENG unit cell: (a) Geometry, and (b) Boundary conditions.

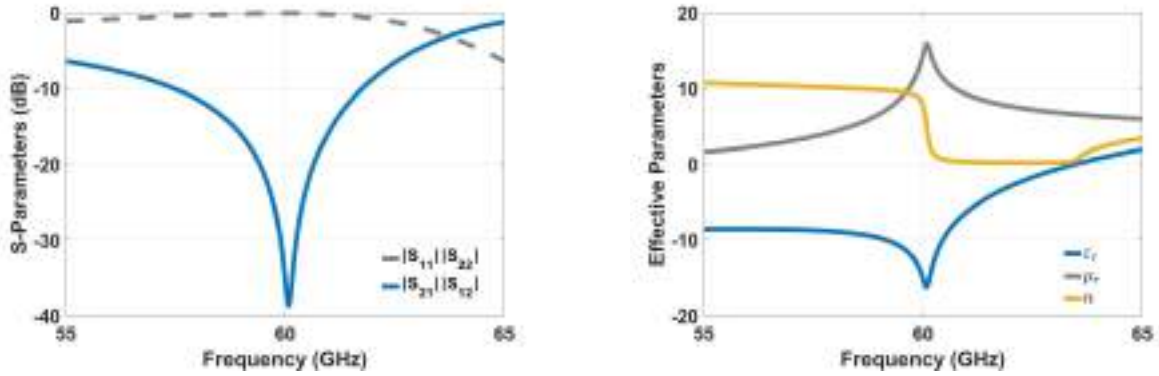
Figure 10a illustrates the simulated transmission coefficient of the proposed ENG metamaterial unit cell. A pronounced stopband behavior is observed around the operating frequency of 60 GHz, where the transmission coefficient reaches significantly low values.

Table 2: Optimized dimensions of the proposed ENG unit cell.

Parameter	r	r_1	r_2	l_1	l_2	g
Value (mm)	1.400	1.130	0.910	0.100	0.150	0.100

This response indicates that the structure effectively inhibits electromagnetic wave propagation within this frequency range. The obtained stopband characteristic demonstrates the capability of the proposed unit cell to suppress undesired electromagnetic coupling, making it suitable for isolation enhancement applications in compact MIMO antenna systems.

The extracted effective electromagnetic parameters of the proposed metamaterial structure are presented in Figure 10b. It can be observed that the effective permittivity ε_r exhibits negative values around the operating frequency, while the effective permeability μ_r remains positive. This electromagnetic behavior confirms the ENG (Epsilon Negative) characteristic of the proposed unit cell. In the ENG region, electromagnetic wave propagation becomes significantly attenuated, resulting in the suppression of surface-wave and near-field coupling effects. Consequently, the proposed metamaterial structure can effectively reduce mutual coupling between closely spaced MIMO antenna elements and improve the overall isolation performance.



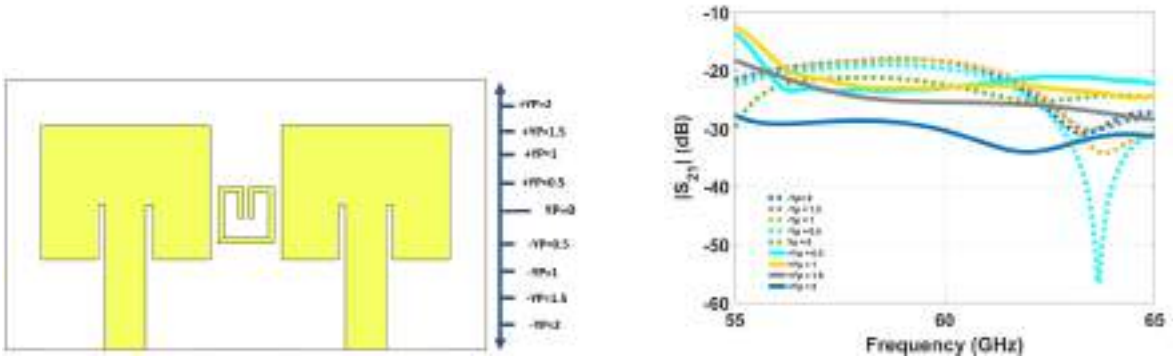
(a) (b)

Figure 10: Simulated response of the proposed ENG unit cell: (a) S-parameters, and (b) extracted effective parameters.

III.6 MIMO Antenna with ENG Metamaterial Isolation Structure

III.6.1 Parametric study of ENG position

Figure 11 presents the parametric investigation of the ENG metamaterial unit cell position along the y-axis and its influence on the transmission coefficient S_{21}. As shown in Figure 11a, the ENG unit cell is displaced along the y-axis to evaluate the effect of its location on the isolation performance of the proposed MIMO antenna. The corresponding transmission coefficients for the investigated positions are illustrated in Figure 11b. From the obtained results, it is evident that the region between $+Y_P = 1.5$ and $+Y_P = 2$ (mm) provides the most significant reduction in mutual coupling around the operating frequency of 60 GHz. Therefore, a refined parametric analysis was performed within this region using smaller position increments. The results indicate that the optimum position is $Y_P = 1.85$ (mm), where the minimum S_{21} value is achieved, corresponding to the highest isolation level. The effectiveness of this optimized position is further confirmed through the comparison results presented in Figure 12b.



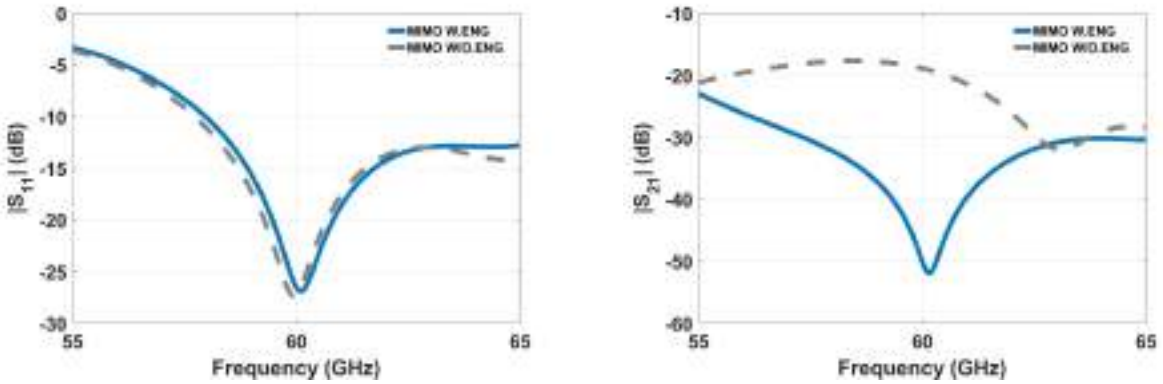
(a) (b)

Figure 11: Parametric study of ENG unit cell position: (a) geometry of proposed MIMO antenna with different ENG positions, and (b) simulated S_{21} for various ENG positions.

III.6.2 Comparative Isolation Analysis with and without the ENG Structure

Figure 12a compares the simulated S-parameters of the proposed MIMO antenna with and without the ENG metamaterial isolation structure. A slight variation in the

impedance bandwidth is observed after integrating the ENG unit cell; however, the antenna still preserves acceptable impedance matching performance around the target frequency of 60 GHz, with S_{11} remaining below the conventional -10 dB criterion. In contrast, a remarkable improvement in the transmission coefficient is achieved after introducing the ENG structure, as illustrated in Figure 12b. The value of S_{21} is significantly reduced from approximately -18 dB to nearly -50 dB at 60 GHz, indicating a substantial suppression of mutual coupling between the closely spaced antenna elements. This isolation enhancement confirms the effectiveness of the proposed ENG metamaterial structure in mitigating electromagnetic interaction and improving the overall MIMO antenna performance.



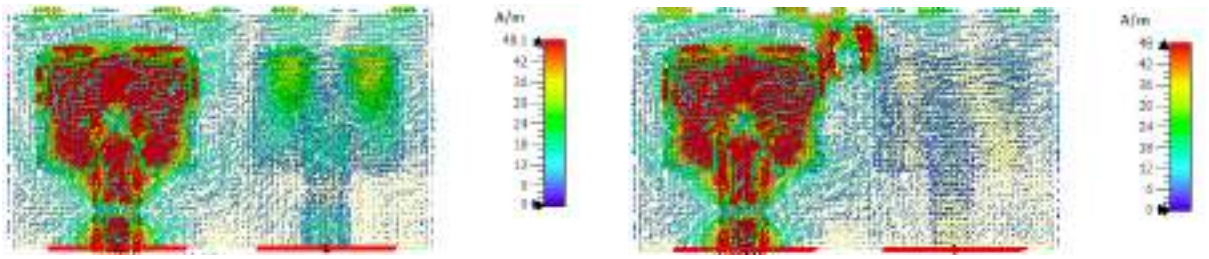
(a) (b)

Figure 12: S-parameter comparison of MIMO antenna with and without ENG structure: (a) S_{11}, and (b) S_{21}.

To further investigate the isolation enhancement mechanism of the proposed ENG metamaterial structure, the surface current distributions of the MIMO antenna with and without the ENG unit cell are compared in Figures 13a and 13b. Without ENG structure, a strong induced current appears on the adjacent antenna element, indicating significant electromagnetic coupling between the radiating patches. The current density is mainly concentrated in the upper region of the antenna structure due to fringing fields and surface-wave propagation.

After integrating the ENG metamaterial structure, the induced current on the neighboring element is considerably reduced, while the current becomes confined around the ENG unit cell. This behavior demonstrates the ability of the proposed ENG structure to suppress near-field interaction and surface wave propagation, thereby providing an effective electromagnetic decoupling mechanism between the antenna elements. As a result,

the mutual coupling is significantly reduced, leading to enhanced isolation performance of the proposed MIMO antenna system.



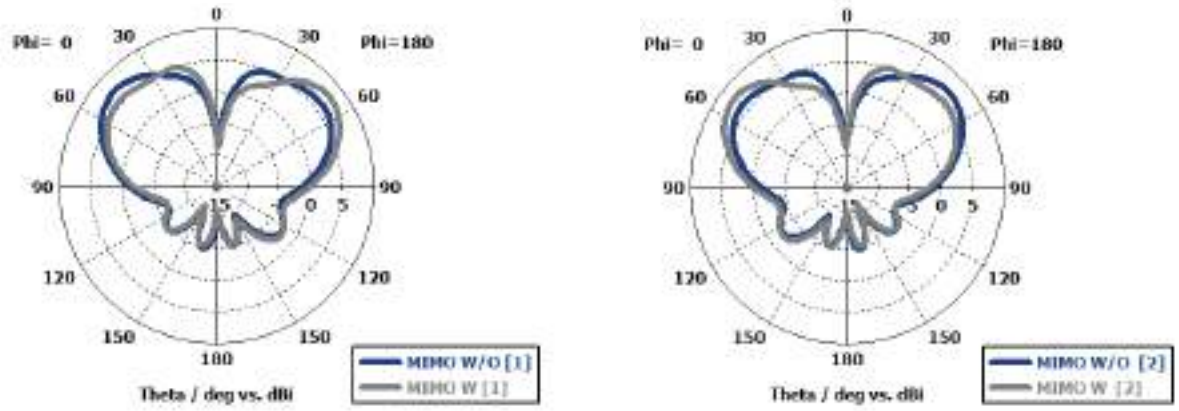
(a) (b)

Figure 13: Surface current distribution of the proposed MIMO antenna: (a) without the ENG structure, and (b) with the ENG metamaterial isolation structure.

Figure 14 presents the two-dimensional radiation patterns of the proposed MIMO antenna for both excitation ports, with and without the ENG metamaterial isolation structure, at the operating frequency of 60 GHz. Figure 14a illustrates the radiation characteristics when Port 1 is excited, whereas Figure 14b corresponds to the excitation of Port 2. It can be observed that the introduction of the ENG structure does not significantly alter the overall shape of the radiation patterns for either port. The principal radiation lobes remain directed toward the broadside direction, preserving the directional characteristics of the antenna. Only minor variations in the side-lobe levels and back radiation are observed after incorporating the ENG unit cell. These results indicate that the proposed ENG metamaterial effectively enhances the isolation performance while maintaining the radiation behavior of the MIMO antenna, demonstrating that the decoupling structure has a negligible impact on the antenna's far-field characteristics.

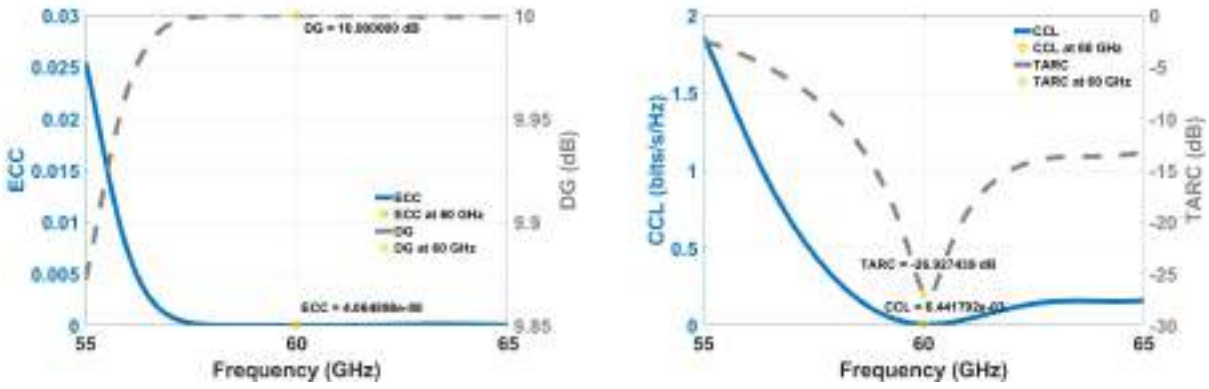
III.7 MIMO Performance Metrics Analysis

The MIMO performance metrics were calculated from the simulated S-parameters using the equations presented previously in Section I.6 of Chapter I. These metrics provide an overall evaluation of the diversity performance, channel capacity, and impedance characteristics of the proposed MIMO antenna system.



(a) (b)

Figure 14: 2D radiation patterns of the proposed MIMO antenna with and without the ENG structure at 60 GHz: (a) Port 1 excitation and (b) Port 2 excitation.



(a) (b)

Figure 15: Simulated MIMO performance metrics of the proposed antenna: (a) ECC and DG, and (b) CCL and TARC.

Figure 15 presents the simulated MIMO performance metrics of the proposed antenna integrated with the ENG metamaterial isolation structure, which were calculated using the formulations introduced previously in Section I.6 of Chapter I. As shown in Figure 15a, the Envelope Correlation Coefficient (ECC) remains approximately 4.06×10^{-8} around the operating frequency, indicating very low correlation between the antenna elements, while the Diversity Gain (DG) reaches 10 dB. In addition, Figure 15b shows that the Channel Capacity Loss (CCL) remains below 0.4 bits/s/Hz, demonstrating negligible degradation in channel capacity, whereas the Total Active Reflection Coefficient (TARC) stays below -10 dB, confirming satisfactory multiport impedance performance. These results are mainly attributed to the ENG metamaterial decoupling structure, which improves the transmission coefficient S_{21} from approximately -18 dB to -50 dB at 60 GHz,

thereby effectively suppressing mutual coupling and enhancing the overall MIMO antenna performance.

Conclusion

In this chapter, the simulation results and performance evaluation of the proposed 60 GHz MIMO antenna system have been presented and analyzed. The single antenna element has demonstrated excellent impedance matching with $S_{11} = -28.51$ dB, a realized gain of 7.17 dBi, and a high radiation efficiency of 92.68% at the target frequency.

The initial 2×1 MIMO antenna, without any isolation structure, has exhibited mutual coupling of approximately -18 dB due to the close edge-to-edge spacing of 1.4 mm. To address this issue, an ENG metamaterial unit cell has been designed and characterized, confirming its negative permittivity behavior around 60 GHz. After integrating the ENG structure at the optimal position ($Y_P = 1.85$ (mm)), the transmission coefficient S_{21} has been significantly reduced from -18 dB to -50 dB, representing a substantial isolation enhancement of 32 dB. The surface current distribution analysis has confirmed that the ENG unit cell effectively suppresses near-field interaction and surface-wave propagation between the antenna elements. Furthermore, the MIMO performance metrics were significantly improved. The ECC approached values around approximately 4.06×10^{-8}, the DG reached 10 dB, the CCL remained below 0.4 bits/s/Hz, and the TARC stayed under -10 dB. These results validate that the proposed ENG metamaterial decoupling structure effectively mitigates mutual coupling and enhances the overall MIMO performance, making it a promising solution for 60 GHz millimeter-wave communication systems.

General Conclusion

This dissertation has successfully presented and analyzed a compact MIMO antenna operating at 60 GHz for millimeter-wave 5G applications. The primary contribution lies in the integration of an ENG metamaterial decoupling structure to enhance insulation between closely spaced antenna elements.

The single antenna element achieved excellent performance with a reflection coefficient $S_{11} = -23.41$ dB, a gain of 7.17 dBi, and a radiation efficiency of 92.68% at 60 GHz. The initial 2×1 MIMO antenna exhibited mutual coupling of approximately -18 dB due to the compact edge-to-edge spacing of 1.4 mm. By introducing the proposed ENG unit cell, the transmission coefficient S_{21} was significantly reduced to -50 dB, representing an isolation improvement of 32 dB.

Consequently, the MIMO performance metrics were substantially enhanced: the ECC remained approximately 4.06×10^{-8}, the DG reached 9.99 dB, the CCL remained under 0.4 bits/s/Hz, and the TARC stayed below -10 dB. These results confirm that the proposed ENG-based decoupling structure effectively suppresses mutual coupling and improves overall MIMO performance.

For future work, the design can be extended to higher-order MIMO configurations, experimentally validated through fabrication and measurement, and adapted to other millimeter-wave frequency bands .

Bibliography

[1] A. Mansour, W. Fathallah, B. B. Salah, and H. Sakli, "Compact mimo antenna design with srr-enhanced isolation for wireless communication," in *2025 International Wireless Communications and Mobile Computing (IWCMC)*. IEEE, 2025, pp. 1336–1341.

[2] L. Assia, C. Maroua, A. Wafa, D. Lotfi, F. Tarek, and B. Rahma, "Millimeter-wave antenna design and analysis for 5g mobile communication," in *2025 3rd International Conference on Electronics, Energy and Measurement (IC2EM)*. IEEE, 2025, pp. 1–6.

[3] B. A. Esmail and S. Koziel, "High isolation metamaterial-based dual-band mimo antenna for 5g millimeter-wave applications," *AEU-International Journal of Electronics and Communications*, vol. 158, p. 154470, 2023.

[4] J. Saini and S. Agarwal, "Design a single band microstrip patch antenna at 60 ghz millimeter wave for 5g application," in *2017 international conference on Computer, Communications and Electronics (Comptelix)*. IEEE, 2017, pp. 227–230.

[5] N. H. Jemaludin, A. J. A. Al-Gburi, R. H. Elabd, T. Saeidi, M. F. Akbar, I. M. Ibrahim, and Z. Zakaria, "A comprehensive review on mimo antennas for 5g smartphones: Mutual coupling techniques, comparative studies, sar analysis, and future directions," *Results in Engineering*, vol. 23, p. 102712, 2024.

[6] B. A. Esmail and S. Koziel, "Design and optimization of metamaterial-based dual-band 28/38 ghz 5g mimo antenna with modified ground for isolation and bandwidth improvement," *IEEE Antennas and Wireless Propagation Letters*, vol. 22, no. 5, pp. 1069–1073, 2022.

[7] F. Raval, Y. Kosta, and H. Joshi, "Reduced size patch antenna using complementary split ring resonator as defected ground plane," *AEU-International Journal of Electronics and Communications*, vol. 69, no. 8, pp. 1126–1133, 2015.

[8] N. Sghaier, A. Belkadi, I. B. Hassine, L. Latrach, and A. Gharsallah, "Millimeter-wave dual-band mimo antennas for 5g wireless applications," *Journal of Infrared, Millimeter, and Terahertz Waves*, vol. 44, no. 3, pp. 297–312, 2023.

[9] D. Barad and D. Sarkar, "Sub-arrays using csrr loaded dual-band microstrip patch antennas for mimo and phased array applications in 6g fr3 band," in *2024 IEEE Microwaves, Antennas, and Propagation Conference (MAPCON)*. IEEE, 2024, pp. 1–5.

[10] J. Yeo and J.-I. Lee, "Design of a high-sensitivity microstrip patch sensor antenna loaded with a defected ground structure based on a complementary split ring resonator," *Sensors*, vol. 20, no. 24, p. 7064, 2020.

[11] M. Singh, S. Singh, and M. T. Islam, "Csrr loaded high gained 28/38ghz printed mimo patch antenna array for 5g millimeter wave wireless devices," *Microelectronic Engineering*, vol. 262, p. 111829, 2022.

[12] I. U. Din, N. A. Abbasi, W. Ullah, S. Ullah, M. A. Ouameur, and D. N. K. Jayakody, "A novel and compact metamaterial-based four-element mimo antenna system for millimeter-wave wireless applications with enhanced isolation," *International Journal of Antennas and Propagation*, vol. 2024, no. 1, p. 7480655, 2024.

[13] P. Tiwari, V. Gahlaut, M. Kaushik, P. Rani, A. Shastri, and B. Singh, "Advancing 5g connectivity: a comprehensive review of mimo antennas for 5g applications," *International Journal of Antennas and Propagation*, vol. 2023, no. 1, p. 5906721, 2023.

[14] T. Raj, R. Mishra, P. Kumar, and A. Kapoor, "Advances in mimo antenna design for 5g: A comprehensive review," *Sensors*, vol. 23, no. 14, p. 6329, 2023.

[15] B. Mekimah, A. Messai, and T. Djerafi, "Amélioration des caractéristiques des patchs microbandes pour les applications ultra large bande." Ph.D. dissertation, Université Frères Mentouri-Constantine 1, 2020.

[16] R. H. Elabd and A. J. A. Al-Gburi, "Super-compact 28/38 ghz 4-port mimo antenna using metamaterial-inspired ebg structure with sar analysis for 5g cellular devices," *Journal of Infrared, Millimeter, and Terahertz Waves*, vol. 45, no. 1, pp. 35–65, 2024.

[17] W. A. Ali, A. A. Ibrahim, and A. E. Ahmed, "Dual-band millimeter wave 2× 2 mimo slot antenna with low mutual coupling for 5g networks," *Wireless Personal Communications*, vol. 129, no. 4, pp. 2959–2976, 2023.

[18] N. Supreeyatitikul and N. Teerasuttakorn, "Improved isolation of a dual-band mimo antenna using modified s-srrs for millimeter-wave applications," in *2020 17th International Conference on Electrical Engineering/Electronics, Computer, Telecommunications and Information Technology (ECTI-CON)*. IEEE, 2020, pp. 388–391.

[19] P. Sharma, R. N. Tiwari, P. Singh, P. Kumar, and B. K. Kanaujia, "Mimo antennas: Design approaches, techniques and applications," *Sensors*, vol. 22, no. 20, p. 7813, 2022.

[20] B. Mekimah, A. Messai, and A. Belhedri, "Gain enhancement of a cpw-fed dipole antenna using a novel multiband planar artificial magnetic conductor surface for uwb applications," *International Journal of Wireless and Mobile Computing*, vol. 21, no. 2, pp. 141–152, 2021.

[21] M. H. Benderradji, S. Berhab, and B. Mekimah, "39 ghz double negative dr-srr 5g mm-wave applications enhancement," in *2024 3rd International Conference on Advanced Electrical Engineering (ICAEE)*. IEEE, 2024, pp. 1–5.

[22] A. Annou, S. Berhab, M. H. Benderradji, F. Chebbara, and B. Mekimah, "Novel eng, mng, and dng metamaterial unit cells for s and c communications," in *2024 8th International Conference on Image and Signal Processing and their Applications (ISPA)*. IEEE, 2024, pp. 1–6.

[23] M. H. Benderradji, S. Berhab, and B. Mekimah, "Performance enhancement of 5g patch antenna at 28 ghz by metamaterial superstrate integration," in *2024 International Conference on Telecommunications and Intelligent Systems (ICTIS)*. IEEE, 2024, pp. 1–5.

[24] R. R. Kanisha and C. Rimmya, "Isolation enhancement in h-plane coupled 5g mimo antenna with tight spacing using miniaturized epsilon negative (eng) metamaterial," *Radio Science*, vol. 60, no. 6, pp. 1–11, 2025.